

polymer papers

Diffraction study of crystalline structure of random copolymers of poly(ethylene terephthalate) and poly(ethylene naphthalene-2,6-dicarboxylate)

X. Lu and A. H. Windle*

Department of Materials Science, University of Cambridge, Pembroke Street, Cambridge CB2 3QZ, UK

(Received 21 February 1995; revised 31 August 1995)

A recent study has indicated that random copolymers of poly(ethylene terephthalate) and poly(ethylene naphthalene-2,6-dicarboxylate) (PET/PEN) can crystallize over the full composition range under the condition of hot-drawing, and that the crystallites formed are based on random sequences of PET and PEN units. This paper is an extension of this study. Wide-angle fibre X-ray diffraction patterns from PET/PEN random copolymers have been recorded using a charge coupled device based three-circle transmission diffractometer, from which reflections on higher layer lines can be observed quantitatively without distortion. These reflections provide additional indications regarding the tilt of the *c*-axis away from the fibre axis, the crystallite thickness and the nature of the non-periodic layer crystallites themselves. The long period has also been measured as a function of composition by small-angle X-ray diffraction. Diffraction modelling of the crystallites using the CERIOUS package confirms the random nature of polymeric chains in the PET/PEN crystallites and enables the level of register between them to be compared with the 'plane start' and the non-periodic layer (npl) models. The most appropriate model is an 'npl', but containing defects in the otherwise perfect sequence register. Copyright © 1996 Elsevier Science Ltd.

(Keywords: crystallization; random copolymer; X-ray diffraction)

INTRODUCTION

Structures of random copolymers of poly(ethylene terephthalate) and poly(ethylene naphthalene-2,6-dicarboxylate) (PET/PEN) have received significant attention in recent years^{1–3} on account of their considerable commercial potential. Of particular interest is the fact that the random copolymers can be crystallized across the complete composition range, and the structure of such mixed crystals, observed using thermal analysis and X-ray diffraction, has been the focus of a recent paper¹. Crystallization of copolymers in the intermediate composition range can be achieved under conditions of hot-drawing, with marked enhancement of crystallinity occurring on subsequent annealing. Fibre diffraction patterns show similar features to those observed in liquid crystalline random copolymers^{4–9}; i.e. well defined off-equatorial peaks, aperiodic layer lines which change position smoothly with composition. The resemblance between these two types of system suggests that the crystalline structure proposed for liquid crystalline random copolymers, i.e. crystallites based on aperiodic sequences which are matched between adjacent chains, may represent a more general class of behaviour covering a wide range of conventional random copolymers.

There have been two main models which describe the

register between aperiodic chains and lead to fibre diffraction patterns in which the layer lines are sampled by discrete reflections. The non-periodic layer (npl) crystallite model, first proposed by Windle and co-workers^{10–13} to explain observations from liquid crystalline random copolymer systems, supposes that the crystallites are based on the lateral matching between short but identical random sequences of monomer units on neighbouring chains; the achievement of such matching requiring a degree of segregation. For each crystallite there is thus a dominant sequence which is matched, but the sequences will vary from crystallite to crystallite. In contrast to the npl crystallite model, the plane start model has been proposed by Biswas and Blackwell^{14–16} to account for crystallinity in the same type of liquid crystalline random copolymers. In this alternative model there is no segregation of identical sequences, but neighbouring random chains are all positioned so that they are held in register only on one single plane in the crystal. While many detailed diffraction studies, including both experimental and modelling work, have been carried out for liquid crystalline random copolymer systems^{4–16}, the distinction between the two models is difficult to draw on diffraction evidence alone. Both the plane start and the npl models imply sampling of the layer lines, which would be continuous for a structure without any register between the chains. The difference¹¹ is that in the case of the plane start model,

* To whom correspondence should be addressed

the register (on the 6 Å scale) decays on moving away from the register plane, and thus the sampled layer line is superimposed on a continuous linear background. In the case of the npl (sequenced matched) crystal the sampling is complete. However, the issue reduces to one of relative intensities rather than distinct, qualitative differences between the diffraction patterns. In the case of thermotropic liquid crystalline polymers other evidence has been brought to bear, such as small-angle diffraction, microscopy of etched surfaces and dark-field transmission electron microscopy, all suggesting that the crystallites are entities more substantial than would be associated with the register between only one (say) ester group on each of the neighbouring random chains, if indeed such minimal register was sufficient to stabilize a crystal in any case.

The fact that the higher order layer lines of PET/PEN fibre diffraction patterns are much more clearly defined than in the case of the liquid crystalline systems examined previously, presents an opportunity to re-address the diffraction question. Further, the conventional nature of the PET/PEN system (as opposed to liquid crystalline) means that the non-crystalline component will be significantly less well oriented than the crystals, if it is oriented at all, and will thus give diffraction intensities which will be less likely to be confused with those from the crystallites.

EXPERIMENTAL

Materials

PET/PEN random copolymers were synthesized from dimethyl terephthalate, dimethyl 2,6-naphthalenedicarboxylate and ethylene glycol. The degree of polymerization of these polymers measured using gel permeation chromatography and viscosity methods is within the range of commercial products, i.e. about 50–150. The sequence distribution has been proven to be nearly random by ^1H nuclear magnetic resonance measurements. The detailed synthesis procedure and characterization of the polymers have already been reported¹.

Sample preparation

Fibres were drawn out from the melt on a hot plate,

and then stretched further in a silicon oil bath at about 10°C above the glass transition temperature (T_g). The draw ratio was in the range of five to eight. The fibres were reheated in a silicon oil bath to the temperature half way between T_g and the melting temperature (T_m), and held at constant length for 4 h before cooling to room temperature. For the diffractometer measurements, a composite sample was prepared by aligning several fibres exactly parallel on a frame.

Wide-angle X-ray scattering (WAXS)

Fibre diffraction patterns of the parallel assemblies of annealed fibres were measured using a charge coupled device (CCD)-based X-ray transmission diffractometer and $\text{Cu K}\alpha$ radiation^{17,18}. In this system fibres were mounted on a three-circle goniometer (horizontal $\theta/2\theta$, vertical ϕ) enabling sufficient reciprocal space to be accessed to acquire a planar section containing the fibre axis. A CCD detector recorded a small area of cylindrical averaged reciprocal space at each position. The images were then combined to produce a composite image of the planar section of reciprocal space. Scans through 2θ from 10° to 50° and ϕ from 0° to 90° were carried out at room temperature. The incident beam was focused using a germanium crystal monochromator, and the sample-detector distance was 72 mm.

Small-angle X-ray scattering (SAXS)

Small-angle X-ray photographs were taken with a Kratky camera, using Ni-filtered $\text{Cu K}\alpha$ radiation. The samples were bundles of annealed fibres, with the fibre axis being perpendicular to the slit collimation system. The distance between the film and the sample was 109.3 mm. Observed small-angle maxima were converted into long periods by simple application of Bragg's law without any specific treatment of background.

Diffraction modelling

X-ray diffraction patterns were simulated using a commercially available package, CERIOUS¹⁹. The simulation process is outlined in Figure 1, while the detailed procedure is described below.

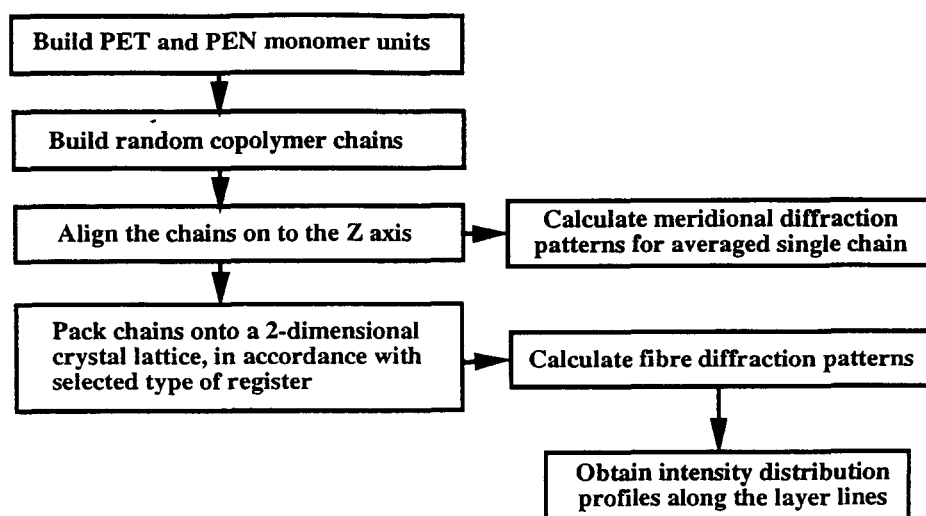


Figure 1 Simulation scheme (see text for detailed procedure)

Molecular parameters of monomer units. The PET chemical repeat unit was built using the molecular parameters (bond length, bond angle and torsion angle) reported for the crystal by Hall²⁰. The conformation in this case is still fairly extended (Figure 2a). The ester groups are rotated about 11° out of the plane of the benzene rings and the CH₂–CH₂ sequence is about 20° from the *trans* conformation. This conformation is slightly different from the recent result reported by Fu *et al.*²¹, although the exact nature of this conformation is not likely to affect our simulation results significantly.

The PEN chemical repeat unit was optimized by MOPAC. A plane conformation was obtained (Figure 2b), which agrees with the experimental result reported by Mencik²².

Geometric parameters of models. The single-chain model was composed of 30 monomer units. No model size correction was used when calculating diffraction patterns.

The dimensions of the three-dimensional crystal models were limited by the capability of the software. The largest three-dimensional model built was eight by eight units in the lateral directions (along the *a*- and *b*-axes), although it is believed that the lateral size of the crystallites in reality may well extend beyond this value. To make the lateral size of the models as large as possible hydrogens were removed from all three-dimensional models, and checks were made to confirm that this action had little effect on the scattering. The crystal thickness in the chain direction was set to both four and five monomer units, in accordance with the indication of random copolymer crystallite thickness obtained from experimental measurement of wide-angle peak widths. The effect of the crystal thickness on simulated diffraction patterns was also examined. On account of the small size of the models, a cylinder model size correction¹⁹ was activated. The effect of the model size and the model size correction method on diffraction patterns will be discussed later with the simulation results.

The interchain distance and packing geometry of the PEN crystal lattice were adopted in all three-dimensional models; it is a reasonable approximation for PET/PEN random copolymers containing 0–60 mol% of ethylene terephthalate (ET) units. In this composition range the crystallites exhibit an 'N' type of structure¹ in which polymeric chains are packed in a lattice similar to that of the PEN crystal. The orientation of the chains within the lattice of the PEN crystal was set so that the plane of the phenyl rings was parallel to (430) (ref. 22).

To approach a random sequence distribution, patterns from 500 random chains were averaged for the single-chain model. The three-dimensional crystal models each contained 64 chains. In cases where chains were identical in an individual model (the npl model), the random pattern was calculated as the average of patterns from all kinds of sequences according to their probabilities. The intensity of the random pattern, $I(R, Z)$, is given by:

$$I(R, Z) = \frac{1}{2^n} \left[\sum_{i=0}^n \sum_{j=1}^{nC_i} (I(R, Z))_{ij} p^i (1-p)^{n-i} \right]$$

where n is the number of units in a chain, $(I(R, Z))_{ij}$ is the intensity from one particular sequence of n units and p is the composition of the random copolymer. If chains

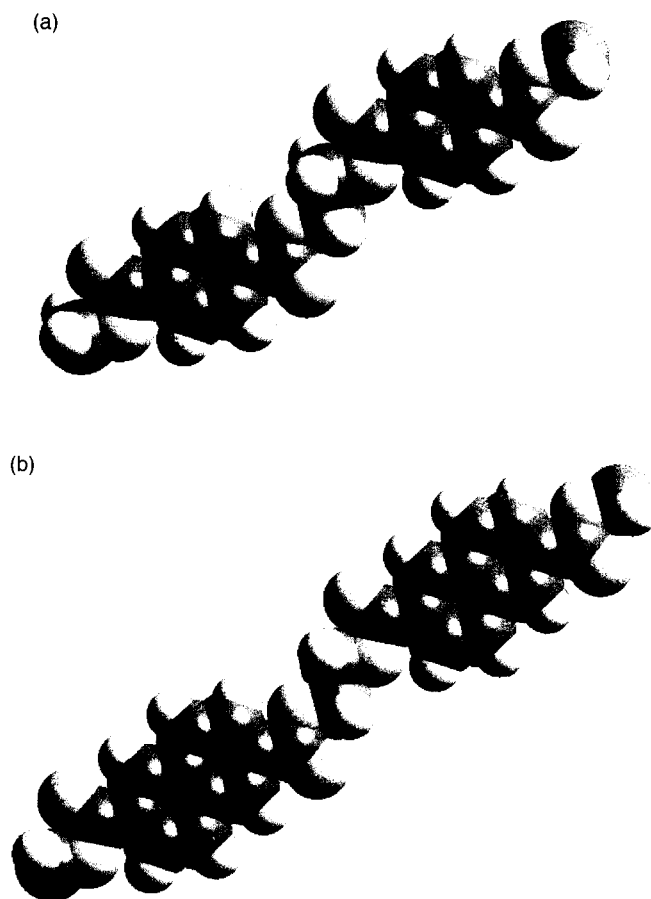


Figure 2 Molecular conformation of (a) the PET unit and (b) the PEN unit used in diffraction modelling

in a model were different from each other (the plane start models), diffraction patterns were calculated by averaging patterns from up to three models (192 chains). The statistical effect of the number of chains on diffraction patterns will be discussed in detail later.

Calculation of diffraction patterns. For periodic structures, the intensity for each (hkl) reflection was calculated using¹⁹:

$$I(hkl) = \left[\sum f_n \cos 2\pi(hx_n + ky_n + lz_n) \right]^2 + \left[\sum f_n \sin 2\pi(hx_n + ky_n + lz_n) \right]^2$$

where f_n is the scattering factor of atom n , and x_n , y_n and z_n are the fractional coordinates of atom n . The summations are over all atoms in the unit cell.

The total cylindrical averaged scattering (fibre diffraction pattern) was calculated using the formula:

$$I(R, Z) = \sum_n \left[\sum_j f_j J_n(Rr_j) \cos(Zz_j - n\phi_j) \right]^2 + \sum_n \left[\sum_j f_j J_n(Rr_j) \sin(Zz_j - n\phi_j) \right]^2$$

where r_j , z_j , ϕ_j are cylindrical polar coordinates of atom j and J_n is the n th order Bessel function. The meridional

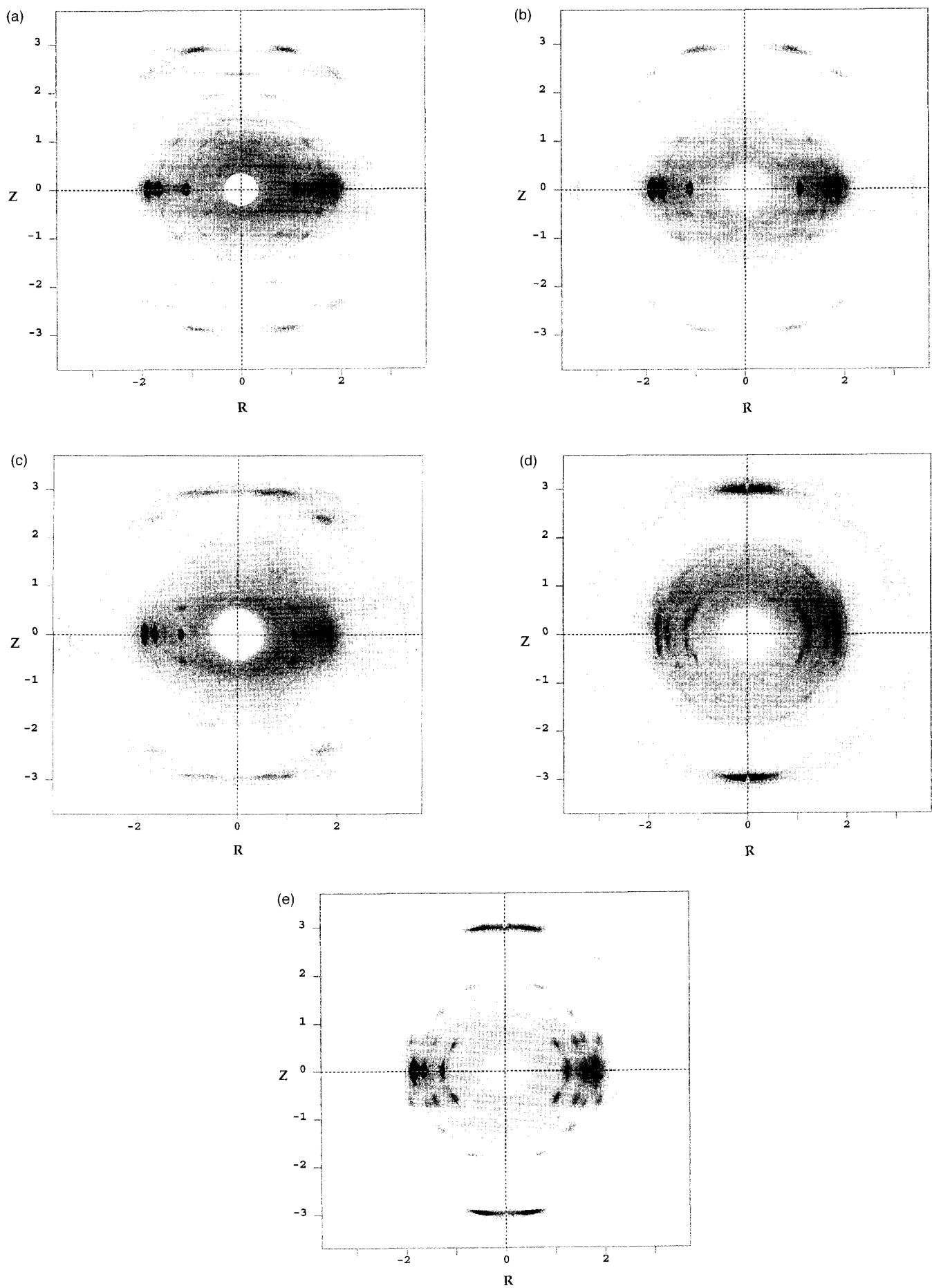


Figure 3 Experimental fibre patterns across the composition range: (a) PEN; (b) PEN/PET, 80/20; (c) PEN/PET, 50/50; (d) PEN/PET, 20/80; (e) PET

section of $I(R, Z)$ is given by:

$$I(0, Z) = \left[\sum_j \phi_j \cos(Zz_j) \right]^2 + \left[\sum_j \phi_j \sin(Zz_j) \right]^2$$

which is the Fourier transform of the projection of the structure onto the Z -axis.

Intensity distribution along layer lines. These intensity profiles were obtained from the CCD diffractometer programmed to scan along the layer lines. Data were gathered from a band $2\theta = 0.57^\circ$ wide centred on the layer line. The intensity distributions along the layer lines of the calculated patterns were obtained for an equivalent band, the distribution being determined by convoluting the line trace at the actual position of the layer line with a smearing function associated with the azimuth width (degree of arcing) of the experimental traces. A background scattering contribution obtained by horizontal scanning at a position mid-way between the layer lines was subtracted from the profiles.

RESULTS AND DISCUSSION

Experimental fibre diffraction patterns

General features of the patterns. Figure 3 shows a series of fibre X-ray diffraction patterns of PET/PEN random copolymers measured using the CCD-based transmission diffractometer. Note that in all the patterns there are some small gaps of the meridian; these are artefacts of the severe geometric constraint associated with exactly meridional information. The patterns have been converted to the cylindrical coordinates of the reciprocal lattice so that layer lines are not distorted and there is no missing information associated with the curvature of the Ewald sphere. In the pattern of PEN, which is typical of a semicrystalline homopolymer (Figure 3a), six layer lines are observed which are composed of distinct (hkl) reflections and are equally spaced. When the ET content increases to 20 mol% (Figure 3b), reflections on the second and third layer lines are rather diffuse although the general features of the pattern do not change very much. When the content of ET units reached 50 mol% (Figure 3c) the reflections of the first layer line are more diffuse but still fairly well defined. However, the second layer line is now basically a continuous lateral streak along which the intensity only changes gradually (unsampled) and the third layer line can hardly be seen at all. The distances between layer lines are clearly aperiodic which, in reflecting the aperiodic nature of the structure along the chain direction, indicates that the crystals are based on random sequences typical of the copolymer as a whole¹. As the content of ET units increases to over 70 mol%, the diffraction pattern features change dramatically in terms of both positions and intensities of reflections on the layer lines although there is no discontinuity in layer line spacing. The ethylene naphthalene-2,6-dicarboxylate (EN) rich phase has been referred to as 'N' type which transforms to 'T' at ET contents above 70%. For the 'T' type of phase, the reflections are not aligned as straight layer lines but are distributed above and below the layer line position. Figures 3d (80% ET) and 3e (PET homopolymer) show this effect. Such

Table 1 The reciprocal lattice coordinates in the chain direction ($\zeta = 2 \sin \theta$) of a particularly distinct high-order layer line, measured for copolymers of different compositions using the CCD-based transmission diffractometer

| Feed composition (ET mol%) | ζ | |
|-------------------------------|-------------------|---------------------------------|
| | 5th | 6th |
| 0 | | 0.71 |
| 20 | | 0.71 |
| 40 | | 0.72 |
| 50 | | $\Leftarrow 0.72^b \Rightarrow$ |
| 60 | | $\Leftarrow 0.72^b \Rightarrow$ |
| 80 | 0.73 ^a | |
| 100 | 0.73 ^a | |

^a The tilt effect has not been corrected for in these data

^b As some of the intermediate layer lines were indistinct in these samples, it was not clear whether the layer line should be designated the 5th or the 6th

behaviour is well understood as a consequence of a tilt between the crystal chain axis and the fibre axis. It has been discussed in the previous paper¹.

An advantage of the WAXS diffractometer technique used in this study over the photographic method is that higher layer lines (fifth and sixth) can be measured without the problems of geometric distortion and information loss which are generally associated with the curvature of the Ewald sphere. Analysis of these reflections will be used specifically to give information about the organization of the aperiodic sequences in the model.

Features of reflections on higher layer lines. Once the ET content decreases below 70% and the 'N' phase forms, the tilt angle goes to zero. However, the layer line, which was the fifth for PET and will become the sixth for PEN, changes only slightly in position with composition as shown in Table 1. Moreover, the pair of strong reflections, $\bar{1}05$ and $\bar{1}\bar{1}5$, for PET, remain on it. Figures 4a–d are a series of diffraction data from the same area of the fibre pattern showing the variations in intensity distribution for the 'N' phase from 60% ET down to the PEN homopolymer. Note how the $\bar{1}05$ and $\bar{1}\bar{1}5$ reflections are sufficiently widely spread on the layer line for the mid-composition ranges to appear clearly separate to the eye. There is a discrepancy in detail between the fibre pattern calculated from the published structure of PEN, where $\bar{1}05$ and $\bar{1}\bar{1}5$ are clearly separate, and the experimental pattern where these strong reflections are again superimposed. The crystallographic implications of this finding have yet to be worked out. However, the persistence of the sharp reflection on a comparatively high-order layer line across the complete composition range is rather significant, especially as lower order layer lines equivalent to about twice the spacing for the mid-composition range are so diffuse as to be difficult to see at all. In any polymer crystal based on ET and EN units, no matter how they are organized along the chains, the fifth order of the ET repeat and the sixth order of the EN repeat have quite similar magnitudes as the ratio of the lengths of the units is close to 5:6, in fact 5:6.11. It is thus possible for planes of this repeat to be near to contiguous throughout the crystal. While the presence of clear sampling of the fifth/sixth order layer lines across the full composition range is not able to act as an indicator of the level of sequence

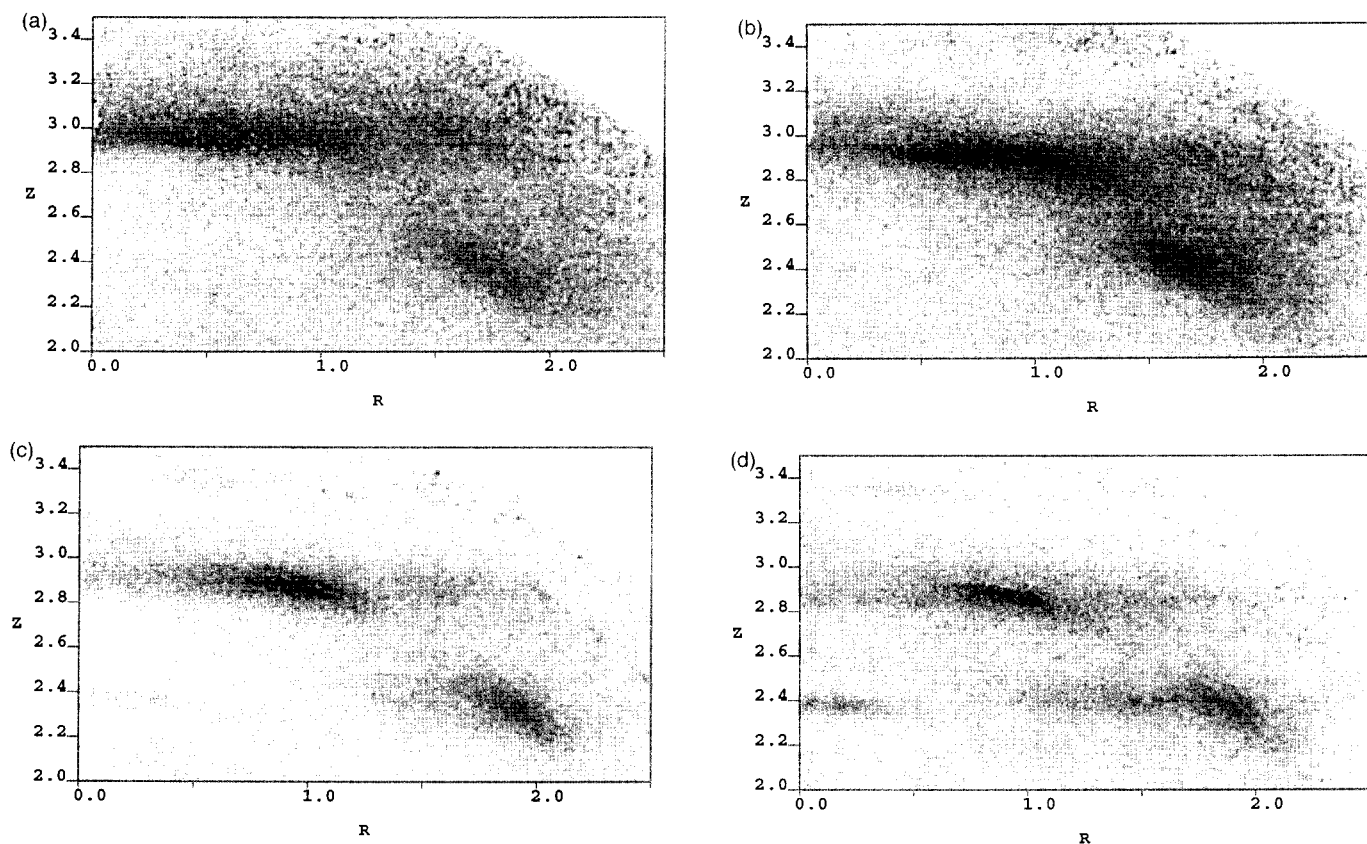


Figure 4 Equivalent regions showing the 5th/6th layer lines [at $z = 2.95$ (approx.)] from experimental fibre diffraction patterns obtained using the CCD-based transmission diffractometer: (a) 60 mol% ET copolymer; (b) 40 mol% ET copolymer; (c) 20 mol% ET copolymer; (d) PEN

matching, it is important to note that the half-width of these reflections in the meridional direction remains essentially unchanged with composition: the half-width is of the order of $2\theta = 2.0^\circ$ which, using the Scherrer formula with the constant set to unity, corresponds to 59 \AA or to five monomer units for the 50/50 composition. We thus have an indication that the neighbouring chains are held in longitudinal register to a resolution of 2 \AA throughout a crystal thickness of at least 59 \AA , and also over a lateral distance (normal to the chain axes) which must approach this value. It should also be borne in mind from ref. 1 that the area of the unit cell normal to the chain axis changes pro rata with composition despite the phase change at 70% ET. There is thus no evidence of any disruption of the crystal as a result of it incorporating both types of unit disposed at random along the chains.

Long period. As a complement to the measurements of crystal thickness from the half-width of the high-order reflection, the crystal long periods were measured as a function of composition by small-angle X-ray scattering. The results are shown in *Figure 5*. It is intriguing to note that the long period is at a maximum in the mid-range of the composition. A possible explanation is that the sequence segregation implicit in the formation of npl crystallites brings with it the implication of 'rejected' material, which could add to the greater amount of polymer between the crystallites. The long period is also about four times greater than the estimated crystal thickness, which would on the assumption of a simple 'two phase' model indicate a crystallinity of 26%, a value in accord with the general appearance of the fibre patterns.

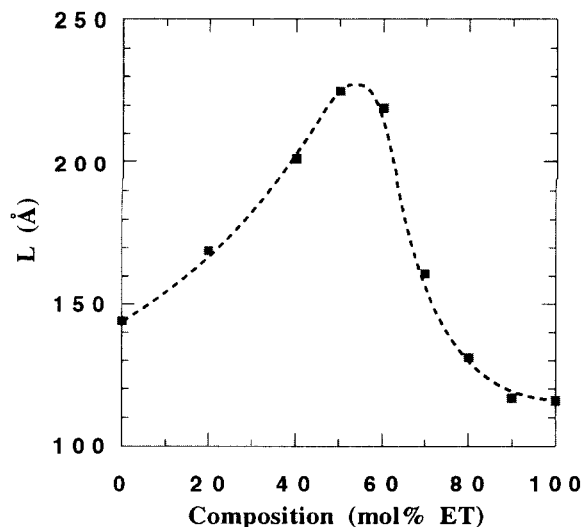


Figure 5 Long period as a function of the composition for the PEN/PET copolymers

Diffraction modelling from single-chain model

As would be expected from elementary diffraction theory, the fibre diffraction pattern calculated from the single-chain model is composed of several lateral (unsampled) streaks, as shown in *Figure 6*. In principle, neither the layer line positions nor the intensity of all but the zero-order line, will be affected by taking the transform of an isolated chain or an assembly of parallel packed chains which lack any longitudinal register. The relative positions and strengths of the layer lines can be

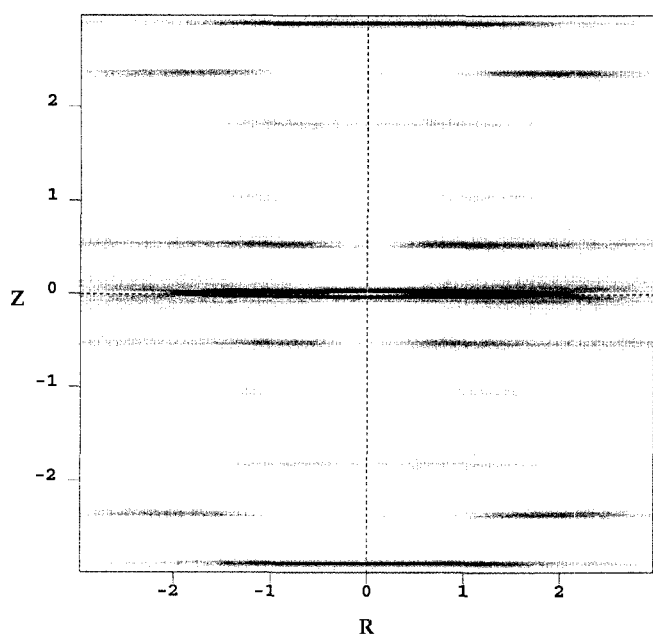


Figure 6 Simulated single-chain fibre diffraction pattern of the PET/PEN random copolymer containing 50 mol% ET

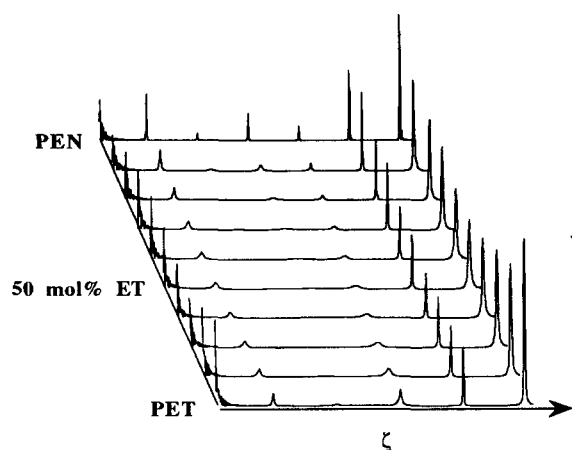


Figure 7 Simulated meridional scans for the PEN/PET random copolymers from single-chain models

compared as a function of composition by taking meridional sections as shown in Figure 7. Note how the number of peaks in the same angular range changes gradually from six for PEN to five for PET. These calculated peak positions are compared with experimental values in Figure 8. The agreement is satisfactory although it should be noted that the model values of ζ are consistently slightly lower than the experimental ones.

Diffraction modelling of three-dimensional crystal models

Model dimensions. The fact that the analysis of peak half-widths has given a measure of the thickness of the crystal provides an important indication of the required size of the models. In the case of the homopolymers there were two methods by which the diffraction could be calculated. The first is the standard method of structure factor determination with the peak sizes being controlled by a 'size correction' which essentially convolutes the point position of the peak with a transform of the crystal

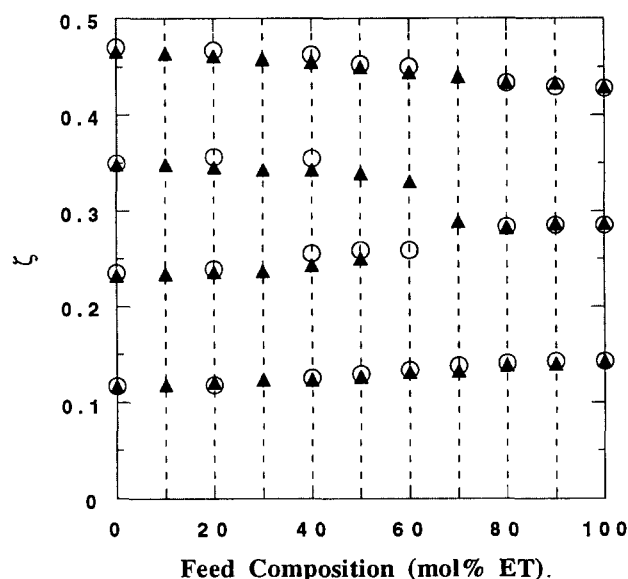


Figure 8 Comparison of reciprocal lattice coordinates of layer lines in the chain direction ($\zeta = 2 \sin \theta$) measured from fibre photographs (O), with the corresponding meridional peak positions simulated for an average single random copolymer chain (▲)

dimensions. The second method is the much more cumbersome one of building a complete model of the required dimensions and transforming the entire crystal. While this method is normally inappropriate, it is the necessary approach for models of crystals based on random chains where there is no lattice. It was therefore considered prudent to compare the two methods for a homopolymer crystal at the outset.

Figure 9a shows the fibre X-ray diffraction pattern for PEN calculated using the structure factor approach, with the reflections smeared in accordance with a crystal thickness of 80 Å in the *c*-direction and lateral dimensions of 100 Å. The resultant pattern resembles the experimental pattern quite closely (Figure 3a). Figure 9b shows the diffraction pattern calculated by transforming the complete model of the same structure having four units in the chain direction and eight by eight units in the lateral directions. The major difference between the two patterns is in the low-angle region where the direct transform of the complete but small crystal gives particle scattering effects which are absent in Figure 9a, where the first stage of the calculation assumed an infinite crystal. Nevertheless, the positions of the higher angle peaks agree well despite the difference in general appearance of the patterns and the presence of some subsidiary maxima in the case of Figure 9b.

While the experimental measurements indicate a crystal thickness of the order of five monomer units, it is sensible to check the influence of the thickness on the predicted patterns. Calculations were made for the plane start model (50 mol% ET), for thicknesses of four, five and six units. The differences amounted only to small changes in peak widths in the *Z*-direction. Due to the limitation of the total atom number in a model, and the need to maximize the number of chains, the crystal thickness in the simulations which follow was set to be four units.

Models consisting of random chains. X-ray fibre diffraction patterns were calculated from a number of

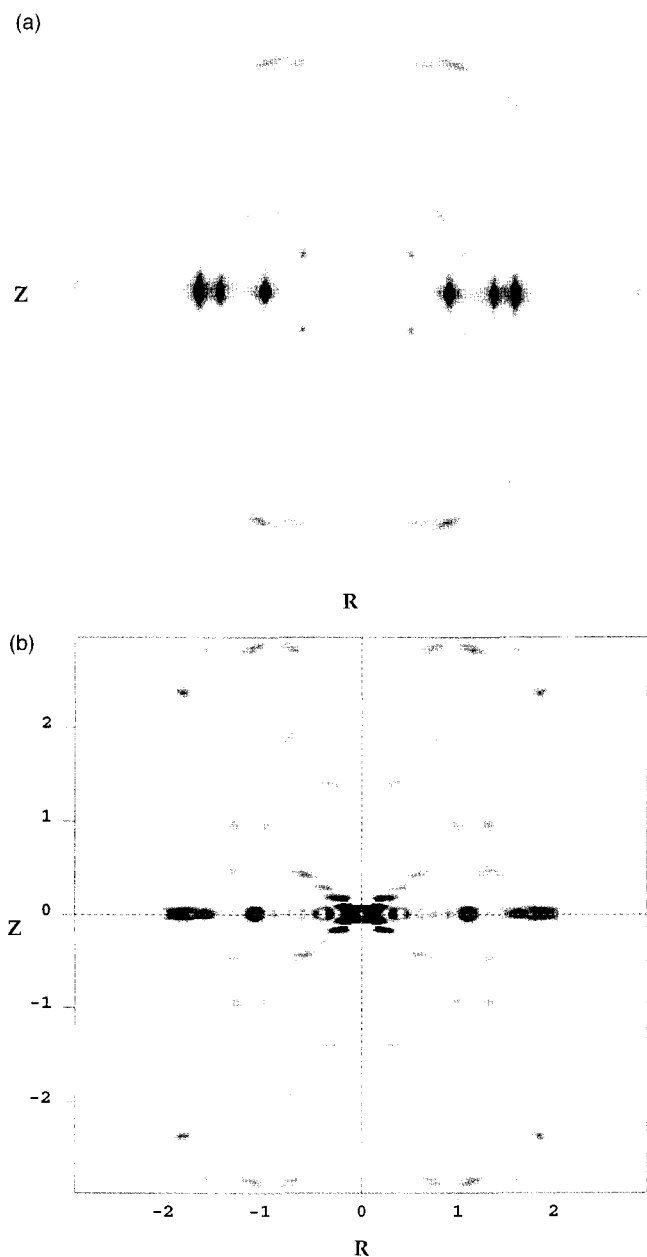


Figure 9 (a) An X-ray fibre diffraction pattern calculated for a PEN crystal using the structure factor approach with the reflections smeared in accord with a crystal thickness of 80 Å in the c -direction and lateral dimensions of 100 Å. (b) An equivalent pattern calculated by transforming the complete model of the same structure with four units in the chain direction and eight by eight units in the lateral directions

three-dimensional crystal models with different chain structures and interchain packing features. The models used in the diffraction modelling are illustrated schematically in Figure 10.

The experimental diffraction pattern from the 50 mol% ET random copolymer (Figure 3c) demonstrates the distinctive diffraction characteristics of a random copolymer system: strong equatorial reflections, well defined off-equatorial peaks and aperiodic layer lines. The 50/50 composition was thus taken as the limiting example of a random copolymer and used predominantly in the diffraction modelling described below.

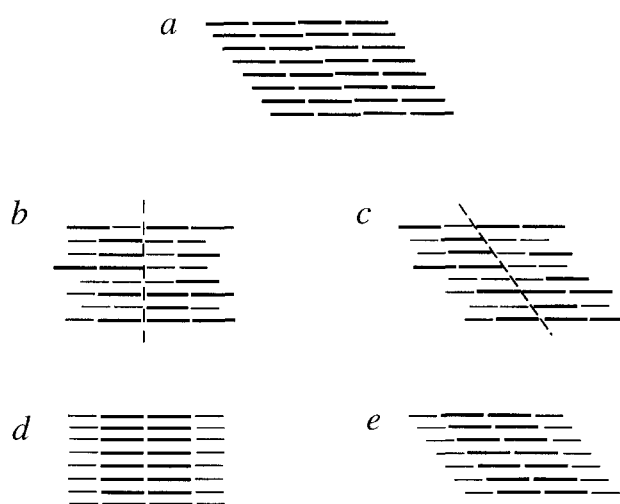


Figure 10 Two-dimensional schematic presentation of the three-dimensional crystal models used for diffraction calculation, in which — represents a PEN unit and — represents a PET unit. (a) The homopolymer model. (b) The plane start model with the central ester group of each sequence level at a plane normal to the chain axis. (c) The same model as (b) except that the matching of the central ester group is at a plane inclined to the chain axis (the $(00l)$ plane of the PEN lattice). (d) The npl crystallite model with random sequences matching at a plane normal the chain axis. (e) The same model as (d) except that the matching is at the $(00l)$ plane of the PEN lattice

Plane start model. With crystals of limited size built from random chains, the question arises as to whether one crystal will give a typical diffraction pattern. In order to explore this matter for the plane start structures, the effect on the predicted scattering of averaging the data from an increasing number of crystals was measured; while it is necessary to average a sufficient number, it is undesirable to perform unnecessary calculations. Figure 11 shows the effect of the number of chains on diffraction patterns for a plane start model which is four units thick in the chain direction and contains 64 chains. An average of two models produces a slightly different pattern, which is little changed for an average of three. The calculations for the plane start model were all the average of three models.

The plane start models, shown in Figures 10b and c, were built by positioning 64 different random chains, each four units long, on a net which was a projection of the a - b plane of the PEN lattice. The chain axes were normal to the net, and the different regimes of interchain register are illustrated in Figure 10. The first type of register considered (Figure 10b) was one in which the central ester groups of the chains were aligned on a plane normal to the chains. Figure 12a shows a diffraction pattern simulated from such an arrangement. In the pattern, the layer line positions are aperiodic and there are three strong reflections appearing on the equator which correspond to the interchain interference. The layer line intensity, however, is largely concentrated on to the meridian, in marked disagreement with the experiment.

Another option is that chains are packed with the central ester group level at the $(00l)$ plane of the PEN lattice (Figure 10c). The diffraction pattern generated in this case is shown in Figure 12b. It can be seen that the general features of this pattern are close to those of the experimental pattern: there are three strong equatorial

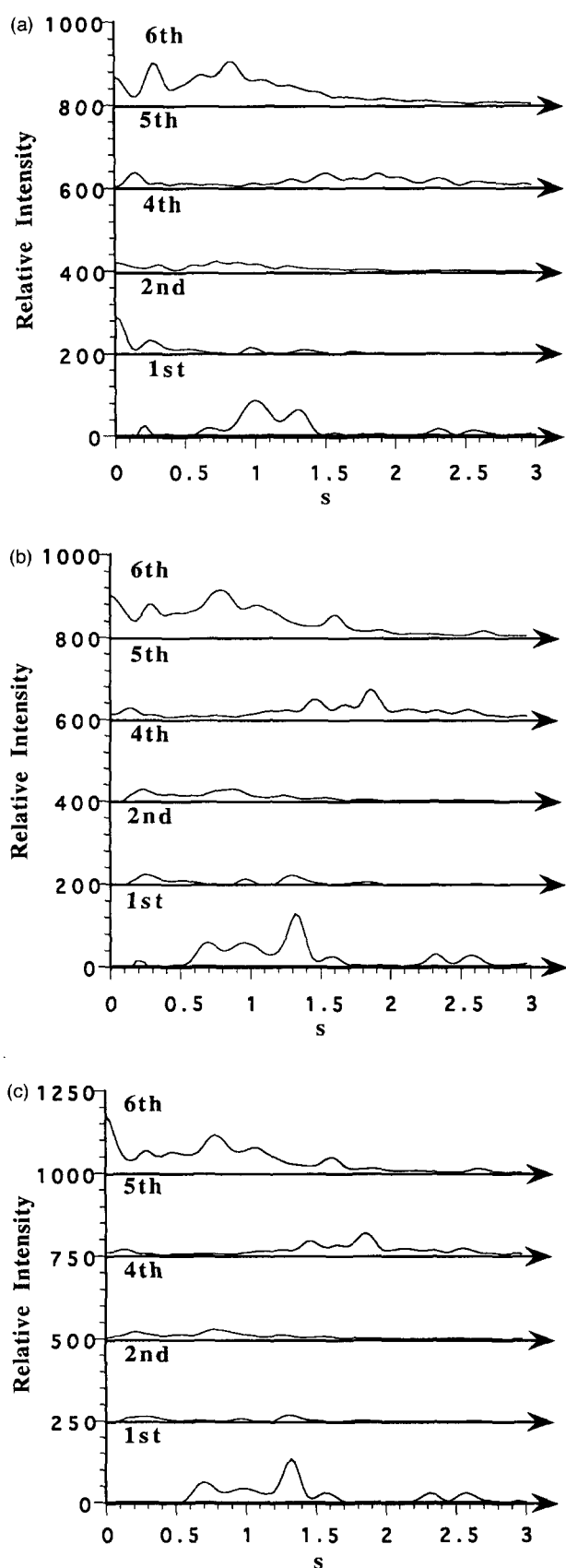


Figure 11 Effect of the number of chains on simulated patterns: (a) the pattern obtained by averaging 64 chains (one crystal model); (b) the pattern obtained by averaging two crystal models; (c) the pattern obtained by averaging three models. The models used are plane start with the central ester group level at the $(00l)$ plane of the PEN lattice. The layer lines are numbered in accordance with the PEN homopolymer

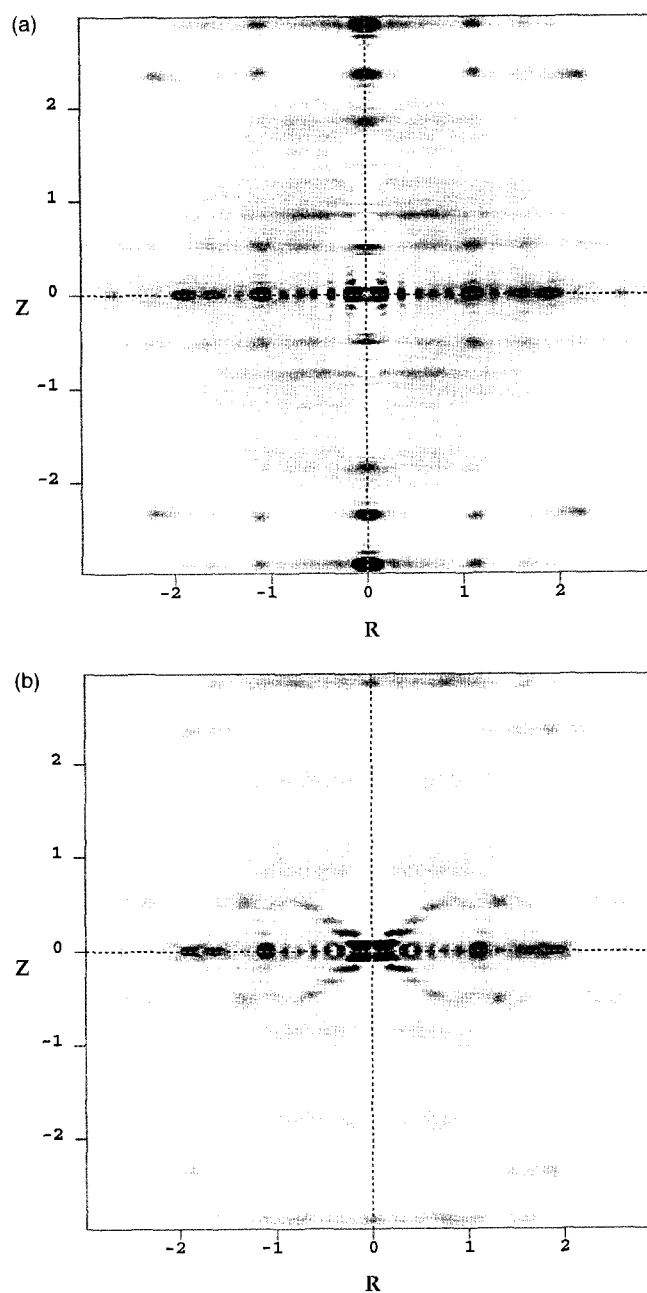


Figure 12 (a) Simulated fibre diffraction pattern of the PET/PEN random copolymer containing 50 mol% of ET. The diffraction modelling was based on the plane start model with the central ester group of each random sequence level on a plane normal to the chain axis (Figure 10b). (b) Simulated fibre diffraction pattern of the PET/PEN random copolymer containing 50 mol% of ET. The diffraction modelling was based on the plane start model with the central ester group of each random sequence level with the $(00l)$ plane of the PEN lattice (Figure 10c)

reflections; the layer line positions are aperiodic; in the off-equatorial region there are relatively high intensities on the first, fourth, fifth and sixth layer lines; while on the second layer line intensity is very low and the third layer line is absent. The main difference from the experimental pattern, however, is that the sampled peaks along the layer lines appear to be superimposed on a continuous line of intensity representative of an isolated chain or a crystal in which longitudinal register is absent.

The fact that the plane start model effectively requires a triclinic unit cell to match the experimental pattern is to be noted.

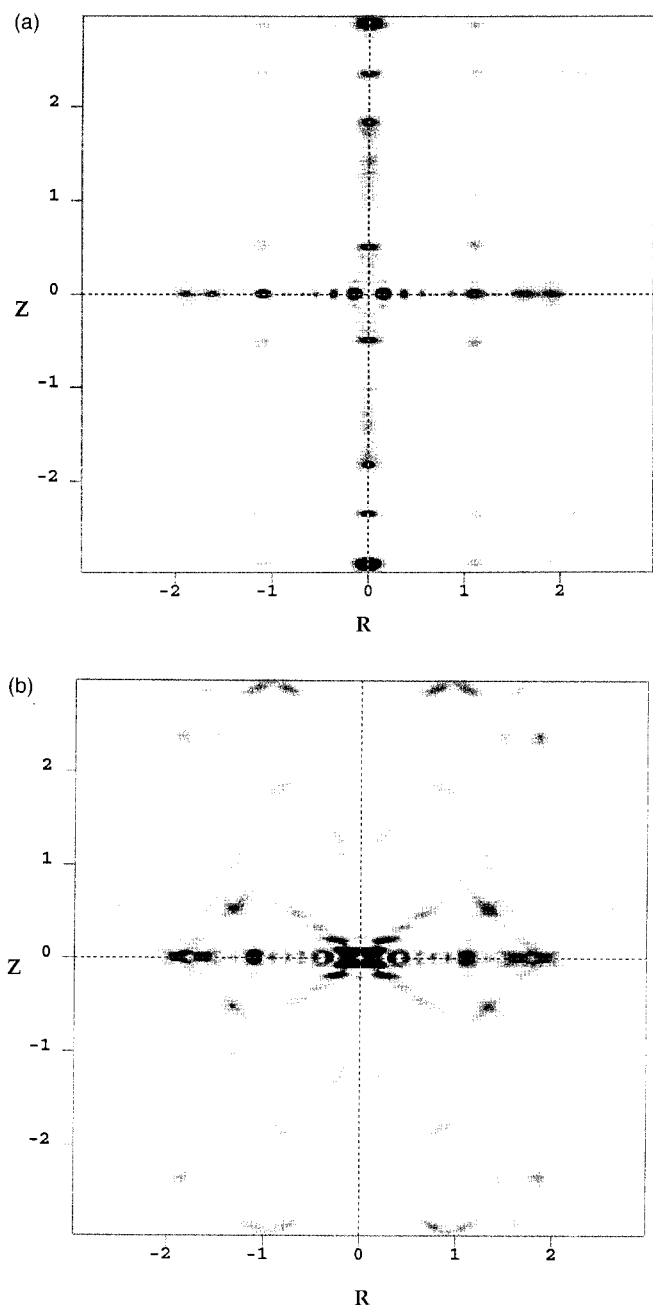


Figure 13 Simulated fibre diffraction patterns of the PET/PEN random copolymer containing 50 mol% of ET. (a) The diffraction modelling was based on the npl crystallite model with random sequences matching at a plane normal to the chain axis (Figure 10d). (b) The diffraction modelling was based on the npl crystallite model with random sequences matching at the (001) plane of the PEN lattice (Figure 10e)

Non-periodic layer (npl) crystallite model. The npl crystallite models were different from the plane start models in that the 64 chains in each model were identical. In directions perpendicular to the chain direction the structure is thus similar to a conventional crystal, but in the chain direction ET and EN units are disposed at random. The statistical fluctuation problem was avoided by averaging the patterns according to the probability of the occurrence of the particular sequence. Again, two types of interchain register were simulated. Figure 13a shows the fibre diffraction pattern simulated from the npl crystallite model with all units matching at a plane normal to the chain axis. As with the plane start model,

the layer line intensities are largely concentrated on to the meridian. Figure 13b shows the fibre diffraction pattern simulated from the npl crystallite model with random sequences matching at the (001) plane of the PEN lattice. The pattern bears considerable similarity with the experimental one although the reflections are, if anything, rather too clearly defined with the complete absence of any continuous layer line background. There are well defined reflections on the first, fourth, fifth and sixth layer lines, which are well related to the features of the experimental pattern.

Intensity distribution along layer lines. The modelling based on plane start and npl registers confirms that the difference in the diffraction patterns of these two models is more quantitative than qualitative. The patterns are essentially the same, although the plane start model gives layer lines in which the continuous background streak is much more in evidence. Figure 14a shows the intensity distributions along the first, second, fourth, fifth and sixth layer lines of the experimental pattern (for 50 mol% ET). These data are compared with three models: (b) zero register (single chain) model (Figure 6), (c) plane start model (Figure 11b), and (d) the npl crystallite model (Figure 12b). It should be noted that the data for the model calculations were obtained from a single line scan along the centre of each layer line rather than a scan covering a narrow band used for the experimental data. This discrepancy could be significant for the higher order layer lines where the arcing of the experimental pattern due to less-than-perfect fibre orientation will tend to smear the experimental scan. In order to facilitate comparison for the sixth order layer line, the scans for the calculated patterns were corrected by convoluting them with a smearing peak corresponding to the combination of arcing and finite width of the layer line scan of the experimental pattern. The comparative scans for this layer line are shown in Figure 15.

Before examining Figures 14 and 15 with a view to deciding on the best model, there is another caveat which should be set down. The model chains were positioned on a net equivalent to the crystal structure of the homopolymer PEN, a structure that is known and accepted in the literature, while earlier work in this project has shown that these parameters are reduced by a few percent for the 50% ET structure¹. The fact that the experimental peaks are displaced to slightly higher scattering angles along the layer lines compared with those predicted by the models is thus entirely consistent.

Comparison of the experimental and model data of Figures 14 and 15 makes it absolutely clear that there is register between neighbouring chains even though the random copolymer chains in the crystal are based on mixtures of the two types of monomer unit. The question, put into focus by looking at the plane start and npl models as rivals, is how much register. The first paper on this work¹ laid some significant groundwork for this system. The fact that the layer line spacings were aperiodic for all random copolymers, the fact that the repeat measured from the position of the first layer line changed smoothly with composition despite the abrupt change in packing at about 70 mol% ET, and the fact that the interchain distances change smoothly with composition at least in the range 0–70 mol% ET, all attest to the mixed composition of the crystals and the

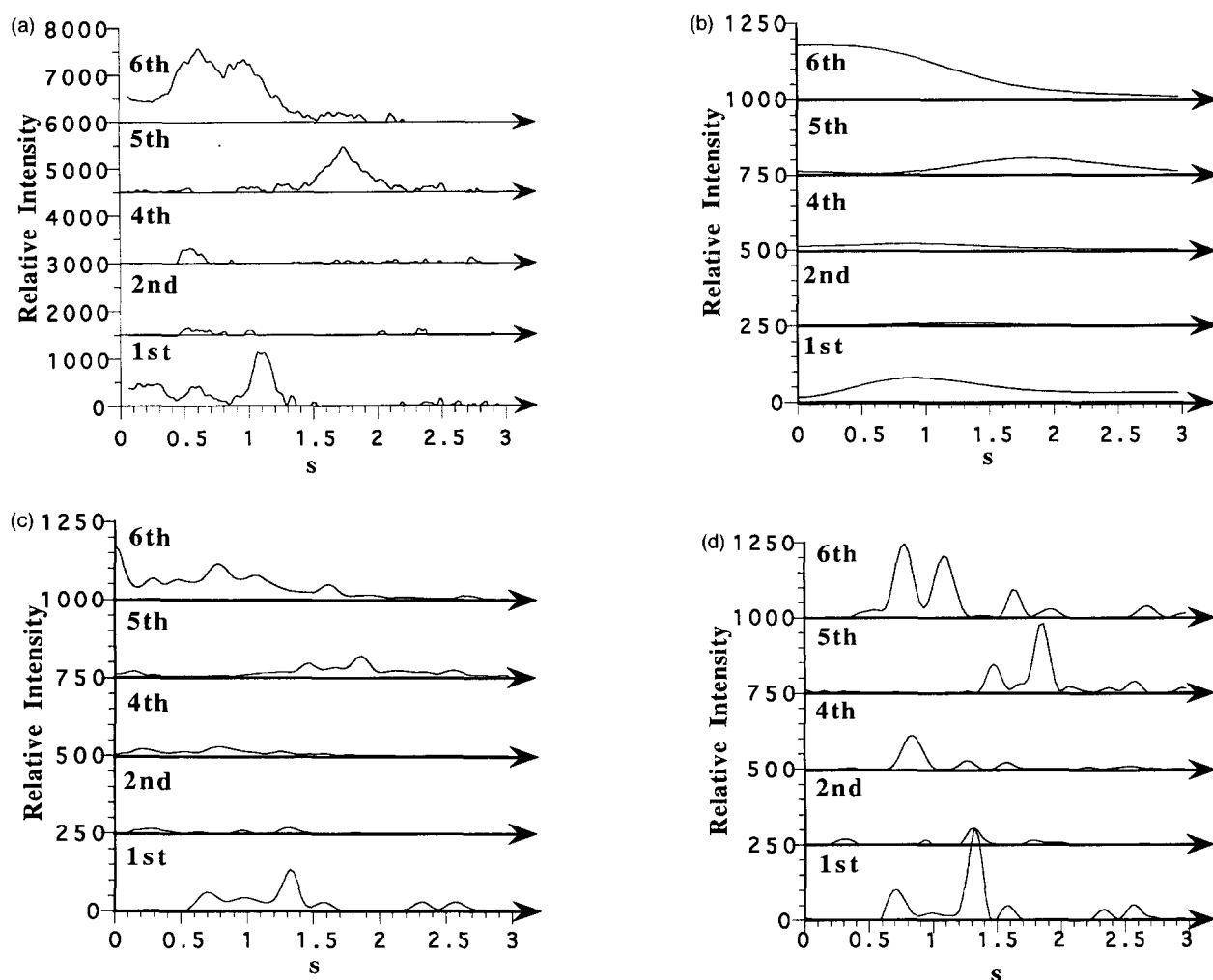


Figure 14 Intensity distributions along layer lines in the experimental and simulated fibre X-ray diffraction patterns of the PET/PEN random copolymer containing 50 mol% ET; s is the cylindrical coordinate of the reciprocal lattice ($4\pi \sin \theta / \lambda$). The experimental profiles were obtained by horizontal scanning of the experimental patterns across a narrow band centre on the layer line. The simulated profiles were obtained by single line scanning along the layer lines of the calculated pattern. (a) Experimental pattern. (b) Pattern generated from the single-chain model. (c) Pattern generated from the plane start model with the central ester group level at the $(00l)$ plane of the PEN lattice. (d) Pattern generated from the npl crystallite model with random sequences matching on the $(00l)$ plane of the PEN lattice

fact that they are based on random copolymer sequences. Yet the new experimental data, reported above, show that the crystals preserve a 2 Å layer repeat over a thickness, in the chain direction, of at least 59 Å. So whatever the particular internal arrangement, it disrupts neither the packing density of the chains nor the axial length of the crystallized units over a distance of at least 60 Å.

Look again at *Figures 14* and *15*. The predictions of the plane start model show discrete maxima along the layer lines, but these are set on a continuous (along the layer line) background, typical of non-registered chains, which is altogether too intense compared with the experimental trace. On the other hand, the predictions of the npl model have no continuous linear background, although this is not completely absent from the experimental data. Thus the plane start model appears to have too little register, while the npl has perhaps too much. In this context it should be remembered that the possible loss of npl sequence matching at the limits of the crystal (in the chain direction) was considered likely at an early stage in the debate, Golombok *et al.*¹¹ proposing in thermotropic random copolyesters than an npl 'core' was

bounded by fringe regions within which the register decayed. While the npl model provides a scheme for register between aperiodic chains, which can be 'softened' on account of defects in the order, the plane start model has no such flexibility. Indeed, it is difficult to see how it can be modified to introduce more register. Furthermore, the model would imply the build-up of mismatch between neighbouring chemical units which would not only mean the loss of favourable interchain ester-ester contacts, but also the need to pack aliphatic and aromatic portions next to each other. The juxtaposition of two chain fragments, one consisting of two ET units and the other of two EN units, held in register at one end would lead to a longitudinal mismatch of some 4 Å at the other.

On the other hand, a problem with the npl model is the necessity of comparatively long-range sequence segregation to enable a group of identical, yet aperiodic, sequences to be gathered into a crystal. While there is evidence that such segregation can occur in the melt in at least one thermotropic copolyester system¹³, there is no such suggestion in this non liquid crystalline system. However, the fact that segregation does occur can also be

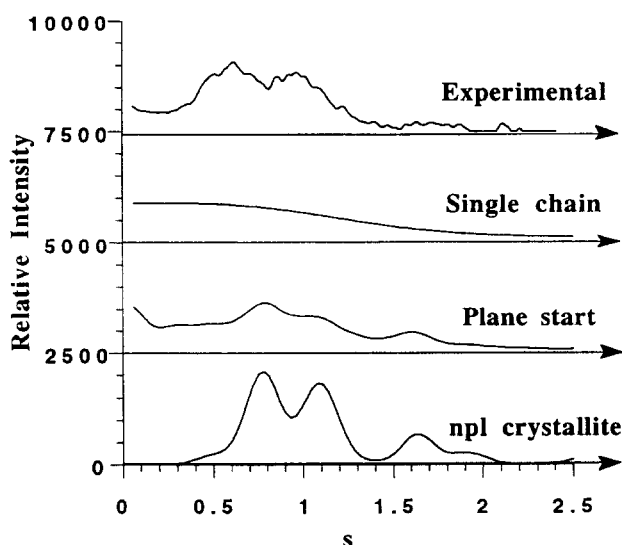


Figure 15 The diffraction profiles on the 5th/6th layer line of the experimental and simulated fibre diffraction patterns from the PET/PEN random copolymer containing 50 mol% ET. The simulated data were obtained by the convolution of a line trace at the actual position of the layer line, as presented in Figure 14, with the projection of the distribution associated with the azimuthal width of the experimental trace

inferred from the plot of axial repeat against composition which is Figure 8 of ref. 1. This plot shows a continuous variation of repeat with composition, yet the relationship is not pro rata: the curve is 'S'-shaped with the variation being gradual towards the limiting homopolymer compositions, but more rapid in the mid-composition range. Such a shape was predicted from the early simple statistical sequence matching schemes¹⁰ and implies that where one or other of the units is in the majority, then the sequences which crystallize are richer still in the dominant unit and they must have segregated. It should also be pointed out that the crystallites in the 50/50 PET/PEN random copolymer system were only well formed after quite extensive annealing of the previously hot-drawn fibres.

We thus consider that the crystallites formed in the PET/PEN system are best described by an npl model containing less-than-perfect sequence register. The exact nature of these imperfections will be the focus of future studies.

CONCLUSIONS

1. Fibre X-ray diffraction patterns of PET/PEN random copolymers obtained using the CCD-based transmission diffractometer can provide full, undistorted sections of reciprocal space and were able to show at least six layer lines.
2. The degree of sampling of the layer lines decreased to a minimum at the third and improved considerably at the sixth, giving a sort of moiré fringe effect in reciprocal space.
3. The diffraction patterns demonstrated conclusively that the crystals were made up of both ET and EN units, that they were at least 60 Å thick and that there was longitudinal register between adjacent chain segments.

4. Comparison of the experimental and simulated fibre diffraction patterns showed that in the PET/PEN crystallites, interchain register is not arranged on a plane normal to the chain axes (the geometries of Figures 10b and d). Agreement was found between the experimental and simulated patterns when the interchain register was organized parallel to the (001) plane of the PEN lattice.
5. The plane start model did not provide sufficient order to match the experimental diffraction pattern. The npl model provided rather too much.
6. The conclusion is that the crystals formed in the system are based on the segregation of like sequences to give non-periodic layers, although the quality of the sequence matching is not perfect. The presence of terminating fringe regions is one possible source of the lack of perfection¹¹, although others are to be explored.

ACKNOWLEDGEMENTS

The authors wish to express their gratitude to A. Willoughby for her expert system management of X-ray facilities used in this work and J. Hobdell for his help with using computer modelling programs. X. Lu wishes to thank the Cambridge Overseas Trust and Trinity College for financial support.

REFERENCES

- 1 Lu, X. and Windle, A. H. *Polymer* 1995, **36**, 451
- 2 Chen, D. and Zachmann, H. G. *Polymer* 1991, **32**(9), 1612
- 3 Cruz, C. S., Balta Calleja, F. J., Zachmann, H. G. and Chen, D. *J. Mater. Sci.* 1992, **27**, 2161
- 4 Gutierrez, G. A., Chivers, R. A., Blackwell, J., Stamatoff, J. B. and Yoon, H. *Polymer* 1983, **24**, 937
- 5 Chivers, R. A., Blackwell, J. and Gutierrez, G. A. *Polymer* 1984, **25**, 435
- 6 Blackwell, J., Biswas, A., Gutierrez, G. A. and Chivers, R. A. *Faraday Discuss., Chem. Soc.* 1985, **79**, 73
- 7 Windle, A. H., Viney, C., Golombok, R., Donald, A. M. and Mitchell, G. R. *Faraday Discuss., Chem. Soc.* 1985, **79**, 55
- 8 Blumstein, A. (Ed.) in 'Polymeric Liquid Crystal', Plenum Press, New York, 1985, pp. 167-181
- 9 Leonid, V. A. *Mol. Cryst. Liq. Cryst.*, 1987, **145**, 31
- 10 Hanna, S. and Windle, A. H. *Polymer* 1988, **29**, 207
- 11 Golombok, R., Hanna, S. and Windle, A. H. *Mol. Cryst. Liq. Cryst.* 1988, **155**, 281
- 12 Hanna, S. and Windle, A. H. *Polym. Prep.* 1992, **33**(1), 288
- 13 Hanna, S., Romo-Urbe, A. and Windle, A. H. *Nature* 1993, **366**, 546
- 14 Biswas, A. and Blackwell, J. *Macromolecules* 1988, **21**, 3146
- 15 Biswas, A. and Blackwell, J. *Macromolecules* 1988, **21**, 3152
- 16 Biswas, A. and Blackwell, J. *Macromolecules* 1988, **21**, 3158
- 17 Hanna, S. and Windle, A. H. *Adv. X-ray Anal.* (Eds P. Predecki et al.) Vol. 38. Plenum Press, NY, 1995
- 18 Hanna, S. and Windle, A. H. *J. Appl. Crystallogr.* 1995, **28**, 673
- 19 'CERIUS Molecular Modelling Software for Materials Research', Molecular Simulations, Inc., Burlington, MA and Cambridge, UK
- 20 Hall, I. H. (Ed.) in 'Structure of Crystalline Polymers', Elsevier Applied Science Publishers, London and New York, 1984, Ch. 2, p. 39
- 21 Fu, Y., Busing, W. R., Jin, Y., Affholter, K. A. and Wunderlich, B. *Macromolecules* 1993, **26**, 2187
- 22 Mencik, Z. *Chem. Prum.* 1976, **17**(2), 78